CHIRAL SYMMETRY

Chiral symmetry: The
π NN coupling should vanish with k_π

H. Sugawara & F. Von Hippel:
"ZERO PARAMETER MODEL OF THE N-N POTENTIAL"
Phys. Rev. 172, 1765 (1968)

π, $\pi\pi$ exchange, NΔ, $\Delta\Delta$ intermediate states

R. A. Bryan, B. L. Scott

ONE-BOSON EXCHANGE N-N POTENTIAL

Phys. Rev, 135, B434 (1964)

σ meson, m = 560 MeV

Chiral dynamics baseline: G.E.Brown & J. W. Durso, PL B 35 B, 120 (1971)

- π, ππ exchange from chiral (LO) Lagrangian:

f_+^0

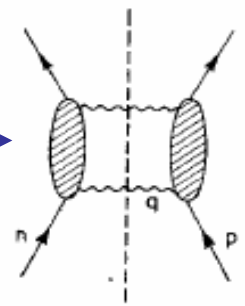

Fig. 1. The two-pion-exchange contribution to the nucleon-nucleon interaction. The wavy lines ~~~ represent pions; the solid lines, nucleons.

PV, chiral coupling

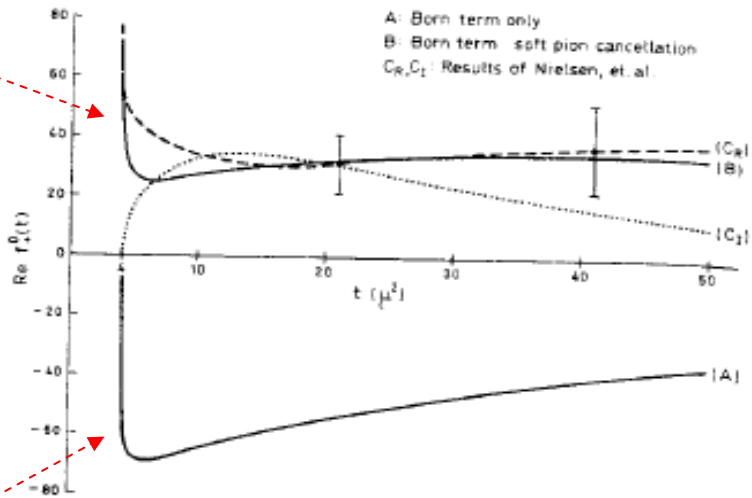

Fig. 2. The f_+^0 obtained from eq. (6) is shown by the solid line ———. The Re f_+^0 and Im f_+^0 obtained in ref. [7] are shown by the dashed ----- and dotted line ....., respectively. Also shown is the f_+^0 obtained from the B^+ of eq. (6.1), neglecting $A^{(+)}$; this is the Born approximation to f_+^0. All amplitudes are plotted in units of the pion Compton wavelength.

Pseudoscalar coupling

NN PHASE SHIFTS

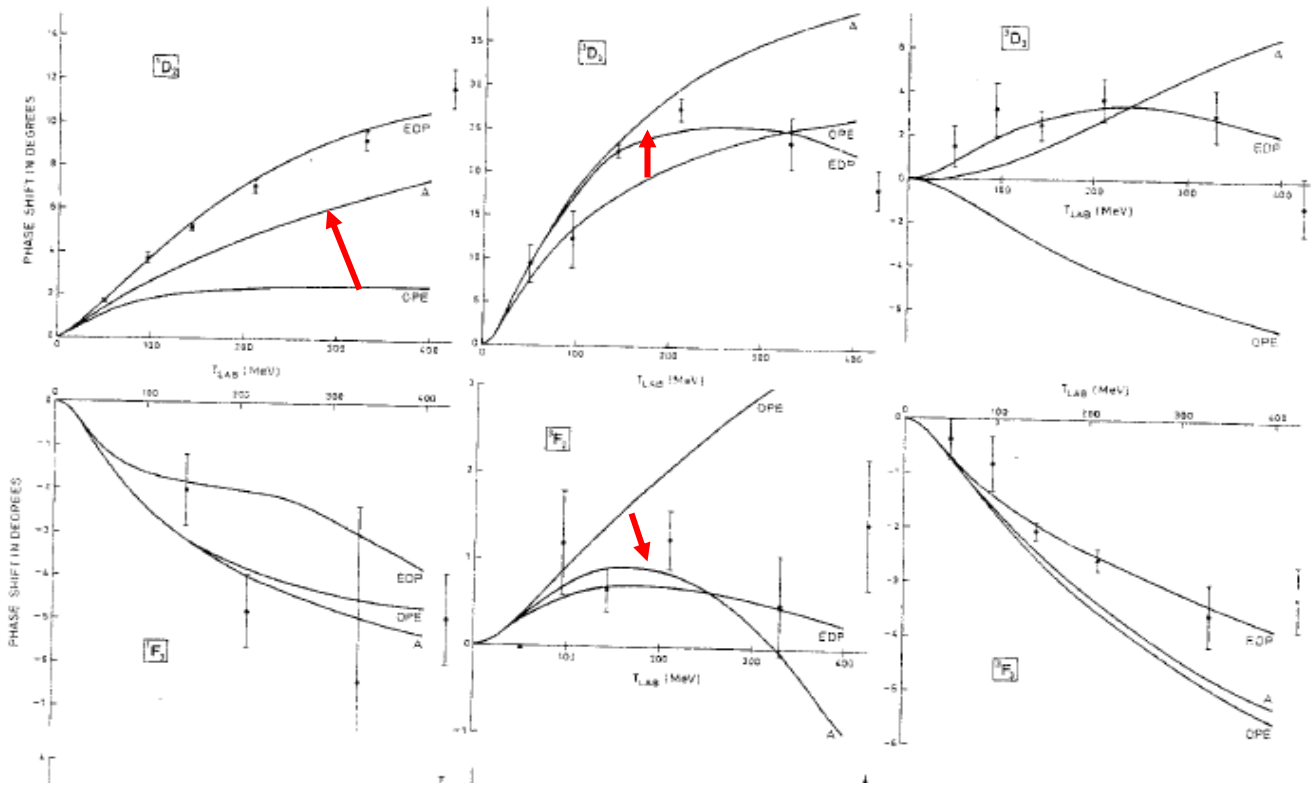

A.D.Jackson & al, NPA 249 (1975) 397

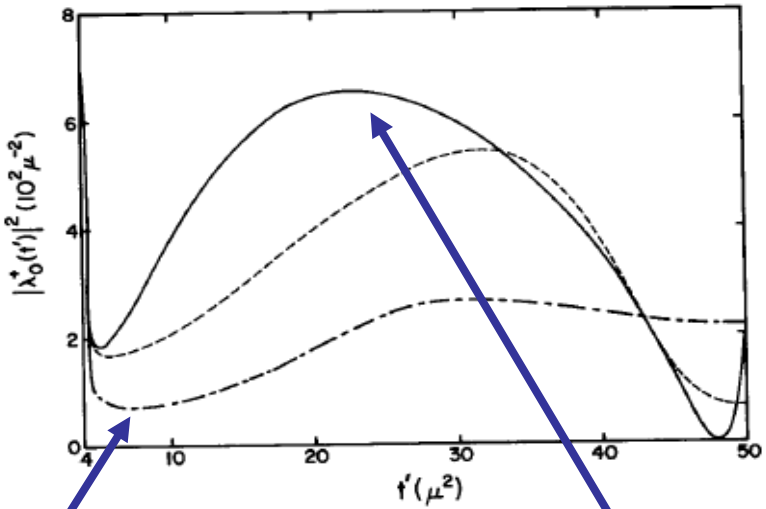

Fig. 5.2.2. The magnitude of λ_0^+ in several models: (i) Nielsen-Oades[33]) (solid curve), (ii) Brown-Durso [34]) (dot-dash curve), and (iii) the model F_0 constructed for the purpose of obtaining a good NN potential (dashed curve).

Brown & Durso

H. Nielsen & G. C. Oades, NPB 49 (1972) 586

PRL **96,** 132001 (2006)

Mass and Width of the Lowest Resonance in QCD

I. Caprini

National Institute of Physics and Nuclear Engineering, Bucharest, R-077125 Romania

G. Colangelo and H. Leutwyler

Institute for Theoretical Physics, University of Bern, Sidlerstrasse 5, CH-3012 Bern, Switzerland

(Received 29 December 2005; published 5 April 2006)

We demonstrate that near the threshold, the $\pi\pi$ scattering amplitude contains a pole with the quantum numbers of the vacuum—commonly referred to as the σ—and determine its mass and width within small uncertainties. Our derivation does not involve models or parametrizations but relies on a straightforward calculation based on the Roy equation for the isoscalar S wave.

$$M_\sigma = 441^{+16}_{-8}\ \text{MeV}, \qquad \Gamma_\sigma = 544^{+18}_{-25}\ \text{MeV}$$

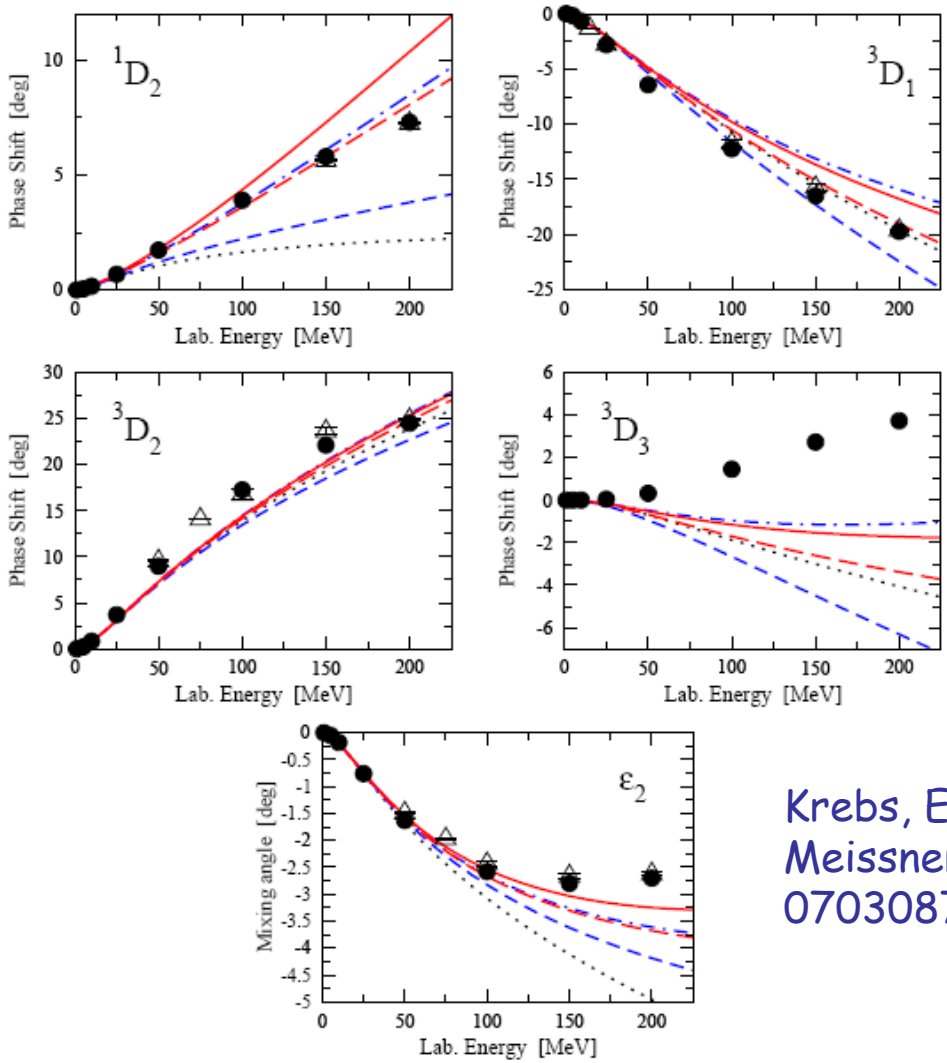

Krebs, Epelbaum & Meissner, nucl-th/0703087

FIG. 7: D–wave NN phase shifts and the mixing parameter ϵ_2. The dotted curve is the LO prediction (i.e. based on the pure OPEP). Long-dashed (short-dashed) and solid (dashed-dotted) lines show the NLO and NNLO results with (without) the explicit Δ-contributions and using the SFR with $\tilde{\Lambda} = 700$ MeV. The filled circles (open triangles) depict the results from the Nijmegen multi–energy PWA [17, 18] (Virginia Tech single–energy PWA [19]).

CHIRAL LONG RANGE PHYSICS

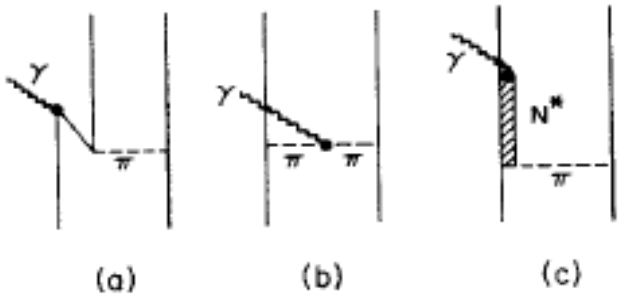

Backward electrodisintegration of the deuteron

J. Hockert et al,
NPA 217 (1973) 14

LO CHIRAL

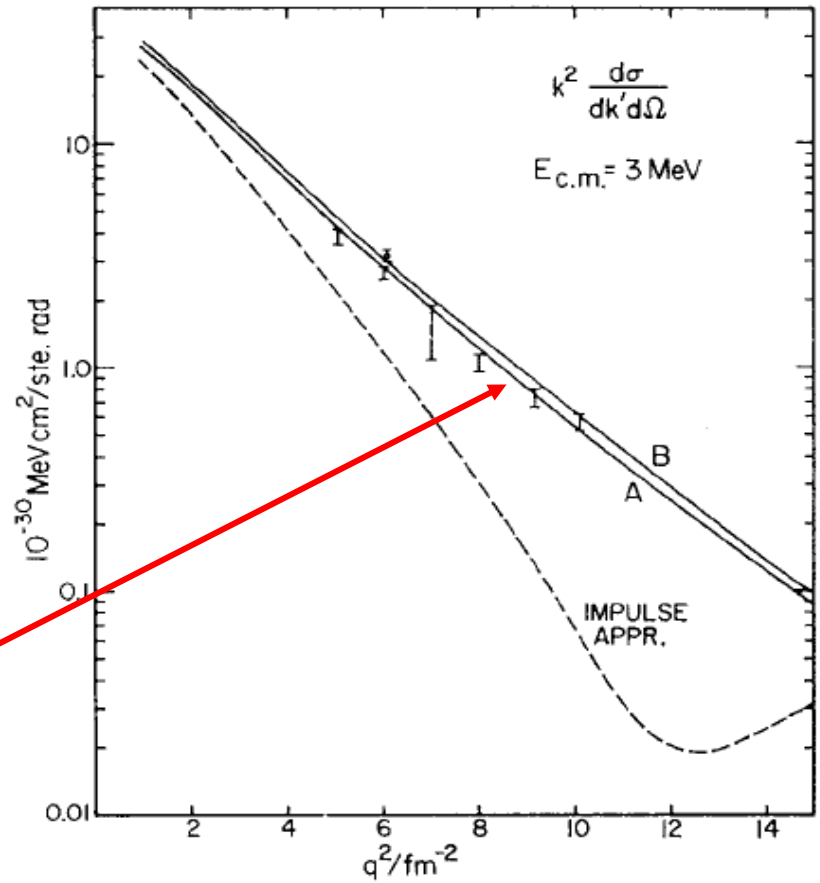

Fig. 8. Cross section for $E_{c.m.}$ = 3 MeV. The curve A shows the cross section when the pion and pair processes are taken into account and the curve B when also the Δ_{33} resonance contribution is included. The data points are the same as in fig. 4.

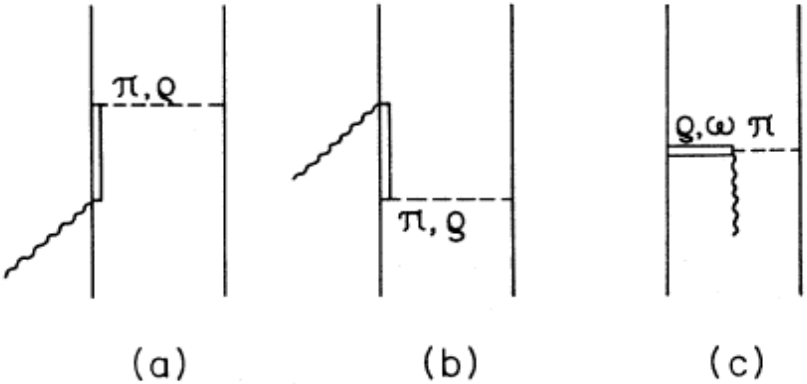

R. Schiavilla & DOR,
PR C43, 437 (1991)

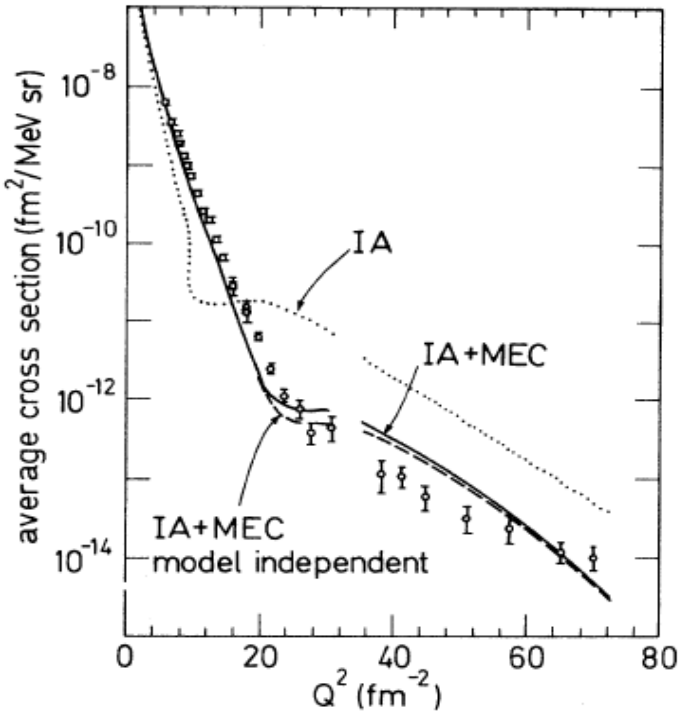

π exchange dominance, because magnetic transition operator scales as $1/m_{ex}$, while interaction scales as m_{ex} !

DEUTERON CHARGE FORM FACTOR

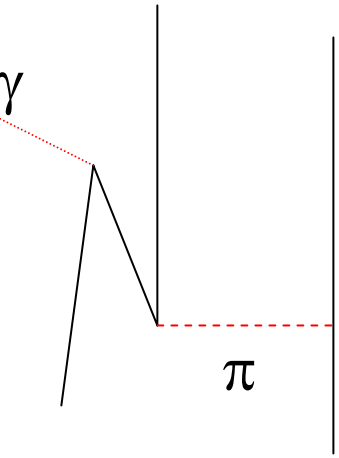

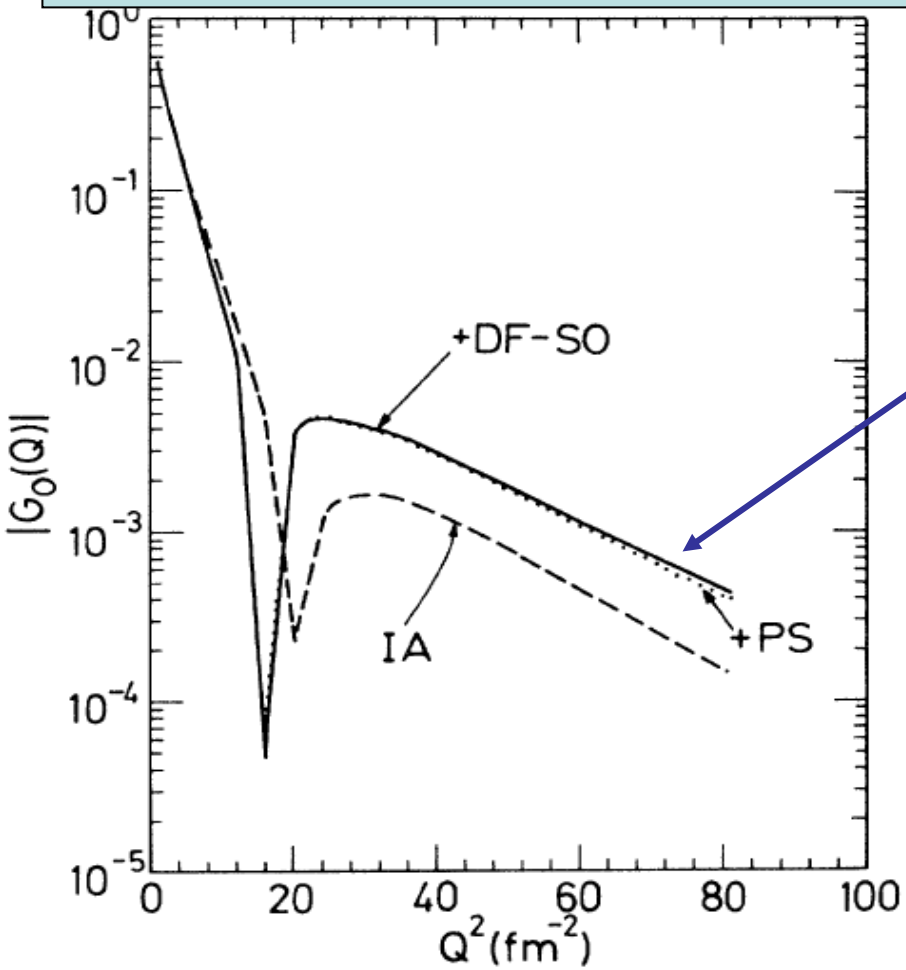

+ exchange current

LO CHIRAL OPERATOR SUPPRESSED, YET PION EXCHANGE DOMINANCE ?

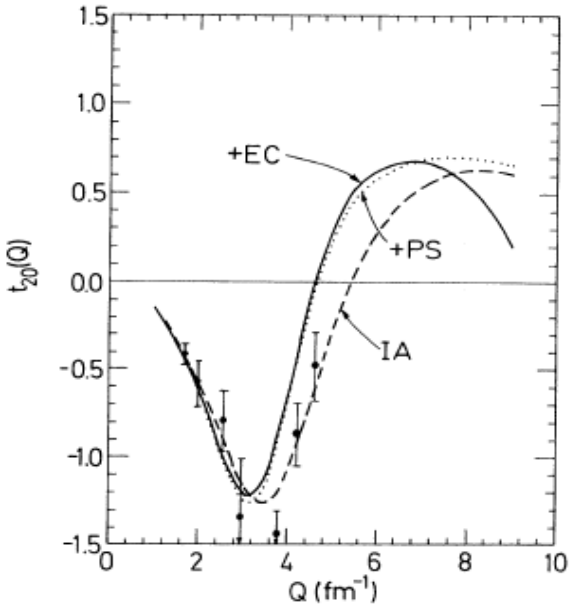

FIG. 21. The deuteron tensor polarization in the impulse approximation (IA) and with the inclusion of the exchange-charge and -current contributions, as well as the Darwin-Foldy and spin-orbit corrections (+EC). The results obtained when the contribution due to the PS ("generalized pion") exchange-charge operator is added to the impulse approximation are also shown (+PS). The Höhler *et al.*[9] parametrization of the nucleon electromagnetic form factors is used. The data points are from Refs. 34, 58, and 59.

R. Schiavilla & DOR, PR C43, 473 (1991)

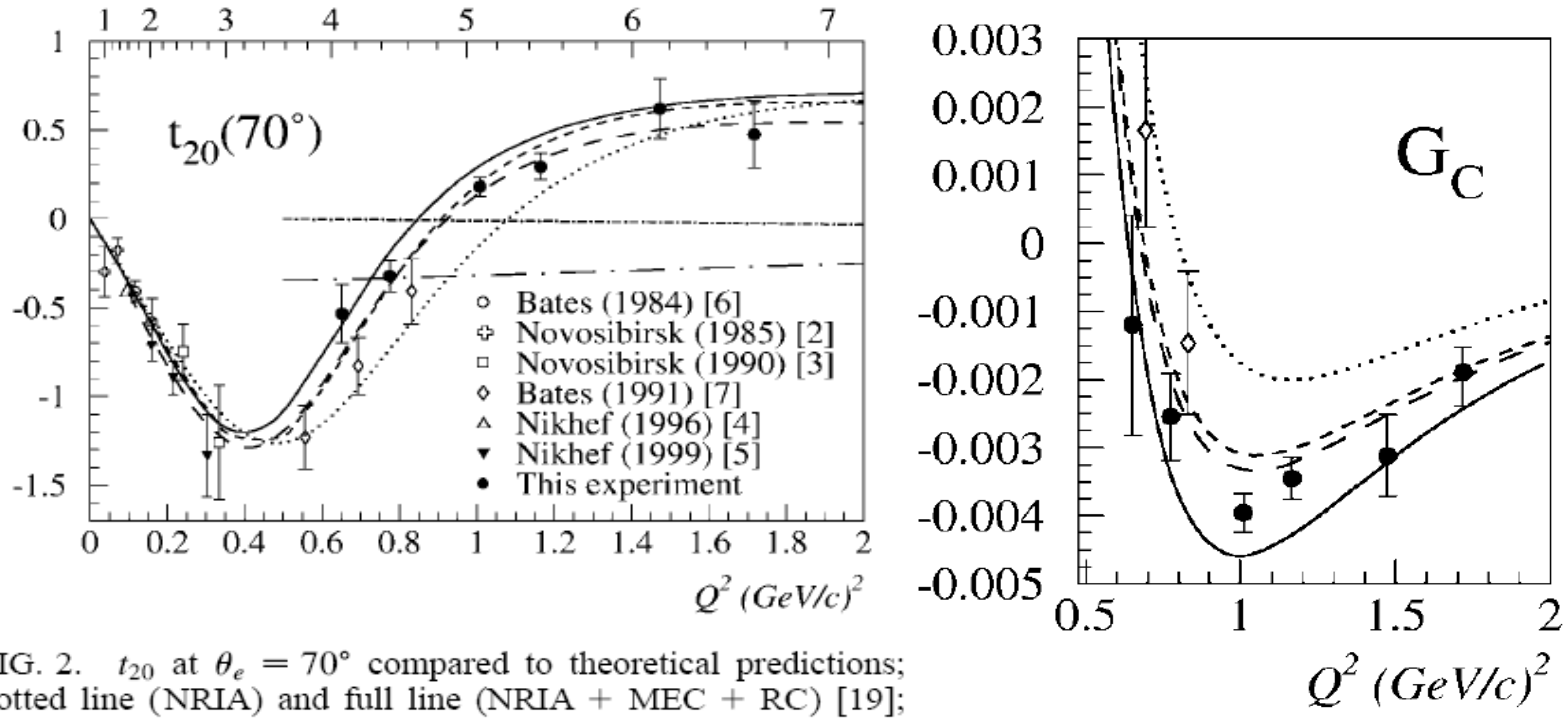

FIG. 2. t_{20} at $\theta_e = 70°$ compared to theoretical predictions; dotted line (NRIA) and full line (NRIA + MEC + RC) [19]; relativistic models with dashed line [21] and long dashed line [22]; pQCD calculations with dash-dotted line [23] and long dash-dotted line [24].

Measurement of Tensor Polarization in Elastic Electron-Deuteron Scattering at Large Momentum Transfer

D. Abbott,[4] A. Ahmidouch,[6,10] H. Anklin,[11] J. Arvieux,[9,12] J. Ball,[2,9] S. Beedoe,[10] E. J. Beise,[3] L. Bimbot,[12] W. Boeglin,[11] H. Breuer,[3] P. Brindza,[4] R. Carlini,[4] N. S. Chant,[3] S. Danagoulian,[10,4] K. Dow,[6] J.-E. Ducret,[2] J. Dunne,[4] L. Ewell,[3] L. Eyraud,[1] C. Furget,[1] M. Garçon,[2] R. Gilman,[4,7] C. Glashausser,[7] P. Gueye,[4] K. Gustafsson,[3] K. Hafidi,[2] A. Honegger,[8] J. Jourdan,[8] S. Kox,[1] G. Kumbartzki,[7] L. Lu,[1] A. Lung,[3] D. Mack,[4] P. Markowitz,[11] J. McIntyre,[7] D. Meekins,[4] F. Merchez,[1] J. Mitchell,[4] R. Mohring,[3] S. Mtingwa,[10] H. Mrktchyan,[13] D. Pitz,[2,3,4] L. Qin,[4] R. D. Ransome,[7] J.-S. Réal,[1] P. G. Roos,[3] P. Rutt,[7] R. Sawafta,[10,4] S. Stepanyan,[13] R. Tieulent,[1] E. Tomasi-Gustafsson,[2,9] W. Turchinetz,[5] K. Vansyoc,[4] J. Volmer,[4] E. Voutier,[1] W. Vulcan,[4] C. Williamson,[5] S. A. Wood,[4] C. Yan,[4] J. Zhao,[8] and W. Zhao[5]

JLAB t_{20} Collaboration, Eur Phys J A7, 421 (2000)

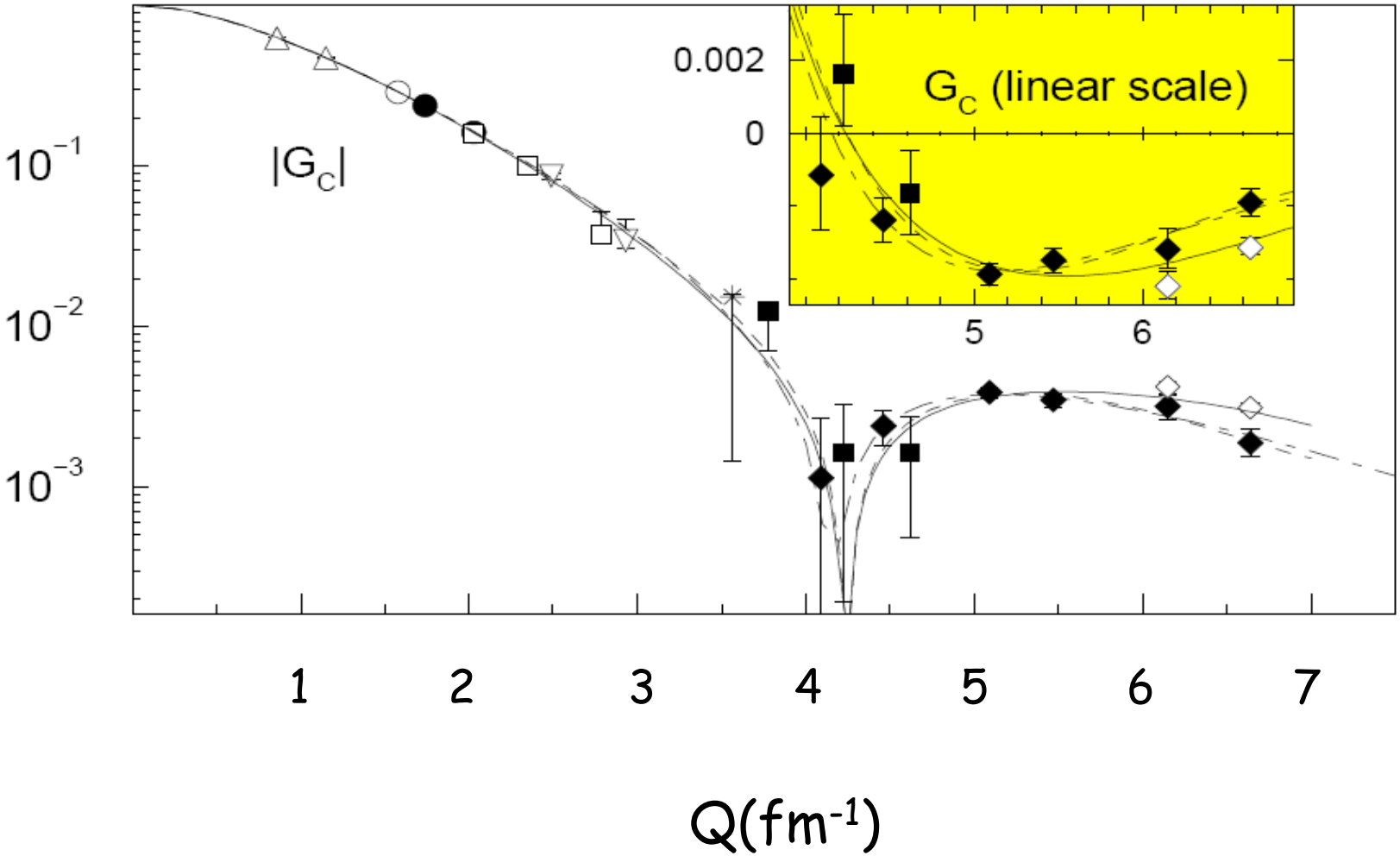

THE SKYRMION

THE SKYRMION

- SKYRME & PERRING 1969: 2-KINK SOL'N TO SINE-GORDON EQN:
  $S_1 \rightarrow S_1$ MAPPING
- SKYRME: HEDGEHOG ANSATZ FOR $S_3 \rightarrow S_3$
- NL SIGMA MODEL + STABILIZER $\rightarrow$ CHIRAL SYM
- WITTEN 1978: DYNAMICAL REALIZATION OF
- LARGE N QCD.
- BARYON PHENOMENOLOGY ~ QUARK MODEL
  $N=\infty$, N=3

Adkins, Nappi, Witten (1982)

CHIRAL HADRON DYNAMICS, QCD & THE SKYRMION

LARGE N : PLANAR DIAGRAMS, gluons ~ qq^- pair lines

π–hadron coupling: $\mathcal{L} = (1/f_\pi)\, A^\mu \cdot \partial_\mu \pi$

ROTATIONS

$A^{ia} = g\, N\, X^{ia}$; $X^{ia} = X_0^{ia} + (1/N)\, X_1^{ia} + \ldots$

Relation to Skyrme model: $X_o^{ia} = (1/2)\, \mathrm{Tr}\{ A \sigma^i A^\dagger \tau^a \}$

SU(4) generators:

$J^i = (1/2) \sum_k^N q_k^\dagger \sigma^i q_k$; $I^a = (1/2) \sum_k^N q_k^\dagger \tau^a q_k$;

$G^{ia} = (1/4) \sum_k^N q_k^\dagger \sigma^i \tau^a q_k$

SKYRME MODEL & NUCLEON SPECTRUM

LOW LYING VIBRATIONAL STATE:

E(1/2*) – E(1/2) = 400 MeV, expt: 500 MeV

L.C.Biedenharn et al, PRD 31, 649 (1985)

I=J states OK,

L.C.Mattis & M. Karliner, PRD 31, 2833 (1985)

HYPERONS IN THE SKYRME MODEL

- STRANGE, CHARM, BEAUTY MESONS BOUND IN THE SOLITON FIELD
- QUANTUM NUMBER TRANSFORMATION: ISOSPIN $\frac{1}{2}$ -> SPIN $\frac{1}{2}$ K,D,B MESONS
- C. Callan & I. Klebanov, Nucl Phys B262,365 (1984),
- N. Scoccola et al realization
- INCORPORATES HEAVY QUARK SYMMETRY

FERMI LAB PRESS RELEASE OCT '06

- $m(\Sigma_b^+) = 5808^{+2.0}_{-2.3}(\text{stat.}) \pm 1.7(\text{syst.})\ \text{MeV}/c^2$
- $m(\Sigma_b^-) = 5816^{+1.0}_{-1.0}(\text{stat.}) \pm 1.7(\text{syst.})\ \text{MeV}/c^2$
- $m(\Sigma_b^{*+}) = 5829^{+1.6}_{-1.8}(\text{stat.}) \pm 1.7(\text{syst.})\ \text{MeV}/c^2$
- $m(\Sigma_b^{*-}) = 5837^{+2.1}_{-1.9}(\text{stat.}) \pm 1.7(\text{syst.})\ \text{MeV}/c^2$

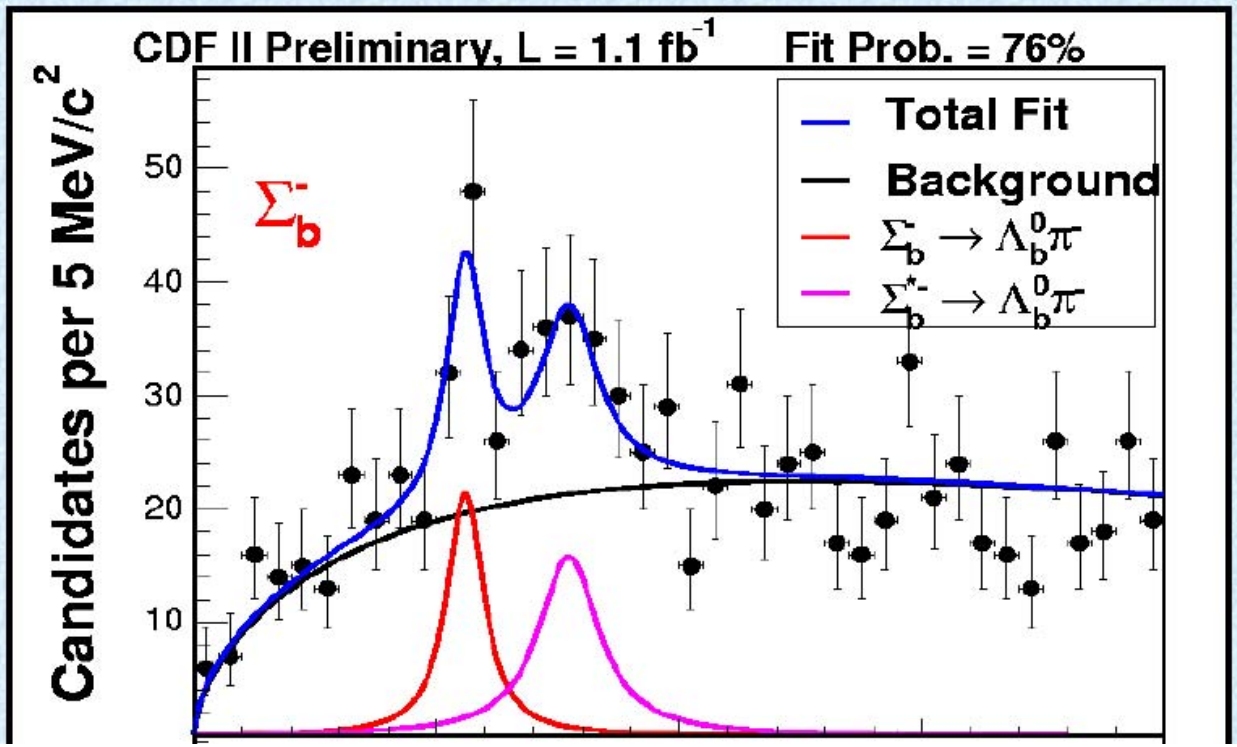

Skyrme: $m(\Sigma_b) = 5806$ MeV, $m(\Sigma_b^*) = 5826$ MeV

M. Rho, N.Scoccola & DOR, Z.Phys.A, 341 (1992)

DOUBLE CHARM HYPERONS

M. Rho et al,
Z Phys A341
343 (1992)

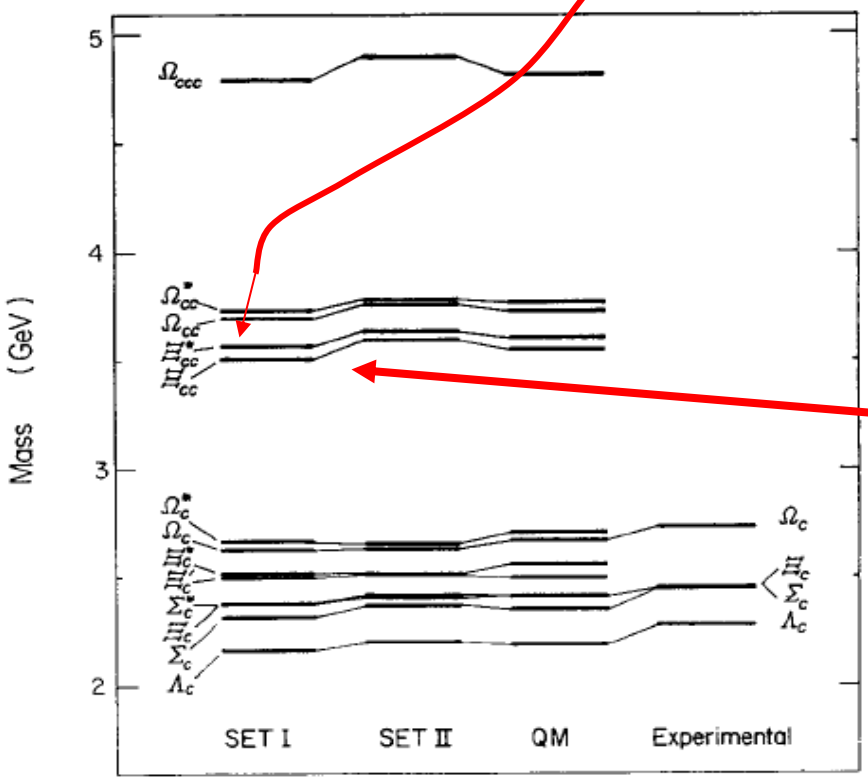

Fig. 1. The energies of the stable charmed and strange-charmed hyperons. The results denoted SET I are those obtained with zero pion mass, and those denoted SET II those obtained with $m_\pi = 138$ MeV. For comparison the quark model results (QM) of [29] are also shown

$\Xi_{cc}^+(3520)$

SELEX,
PLB 628
(2005) 18

$\Xi_{cc}^{++} \sim 3460$

SKYRME MODEL ~ QUARK MODEL
FOR GROUND STATE BARYONS

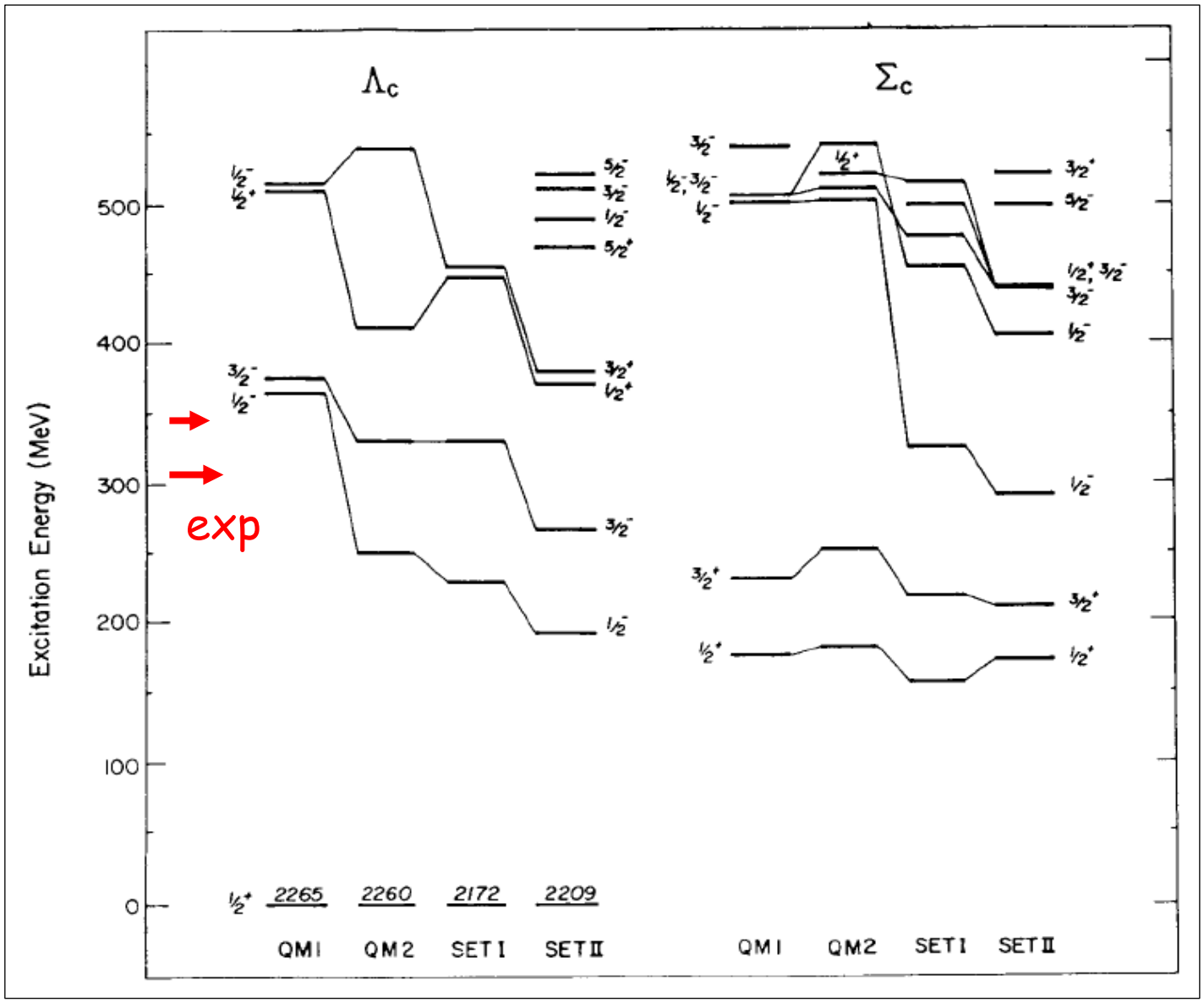
Λc
Σc
Excitation Energy (MeV)
500
400
300
200
100
0
exp
½⁻
½⁺
5/2⁻
3/2⁻
1/2⁻
5/2⁺
3/2⁺
1/2⁺
3/2⁻
1/2⁻
½⁺ 2265 2260 2172 2209
QM1 QM2 SET I SET II
3/2⁻
½⁻, 3/2⁻
1/2⁻
1/2⁺
3/2⁺
5/2⁻
1/2⁺, 3/2⁻
3/2⁻
1/2⁻
1/2⁻
3/2⁺
3/2⁺
1/2⁺
1/2⁺
QM1 QM2 SET I SET II

NUCLEI AS SKYRMIONS

Nucleons: $U(\mathbf{r}) = \exp\{i F(r)\, \pi\cdot\mathbf{r}\}$; F(r): soln to 2nd order diff. eqn

Nuclei: B=2 ground state solution has axial symmetry

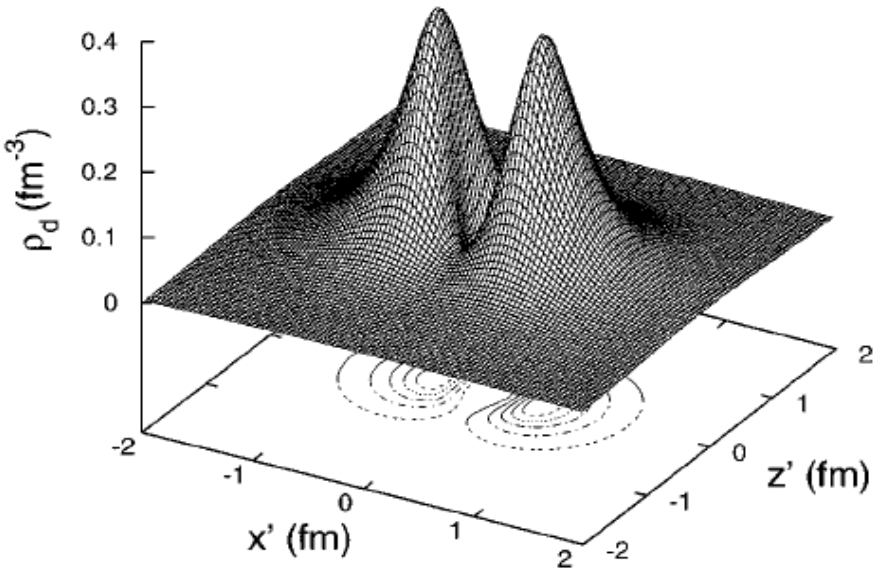

FIG. 4. The deuteron density $\rho_d^0(x',z')$ obtained from the Argonne v_{18} model. The peaks are located at $z'=0$ and $x'=\pm d/2$.

B

$M_d=0$

$\rho_d^0(\mathbf{r}')=0.24\ \mathrm{fm}^{-3}$ (B)

J.L.Forest et al,
PRC 54, 646 (1996)

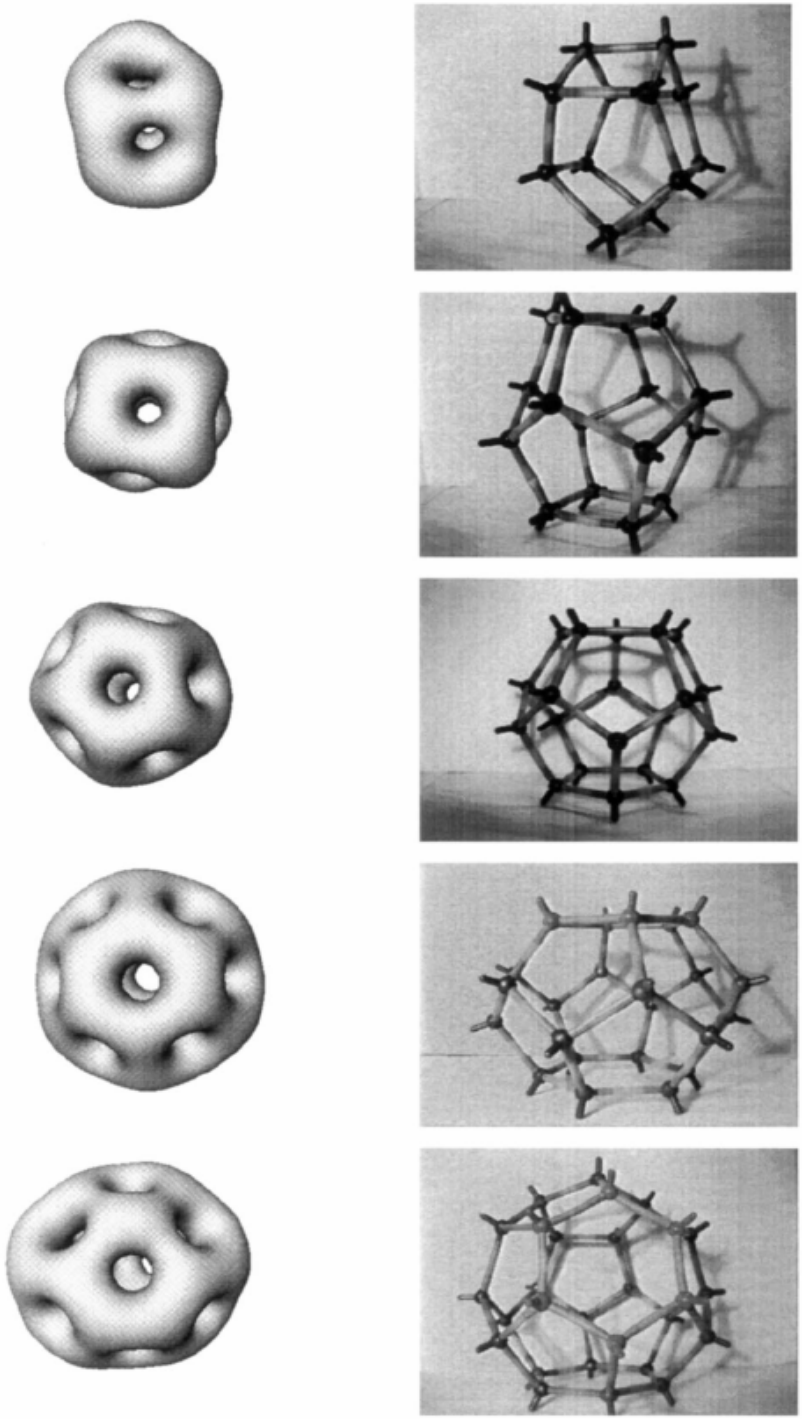

R. A. Battye & P. M. Sutcliffe,
PRL 79, 363 (1997)

FIG. 1. Skyrmions of charge 5 to 9; on the left baryon density isosurfaces (to scale) with 5 at the top and 9 at the bottom and on the right wire frame models of the corresponding solids. Note that the wire frame models are not to scale and have different orientations to the baryon density plots.

SKYRME'S PRODUCT ANSATZ

$U(r;r_1,r_2) = U(r-r_1)\,U(r-r_2)$

$L = L_1 + L_2 + L_{int}$ $\pi\pi$ exchange interaction, realistic isospin dependent interaction components

Current density:

$j = j_1 + j_2 + j_{int}$

Deuteron magnetic form factor

E M Nyman & DOR,
PRL 24, 3007 (1986)

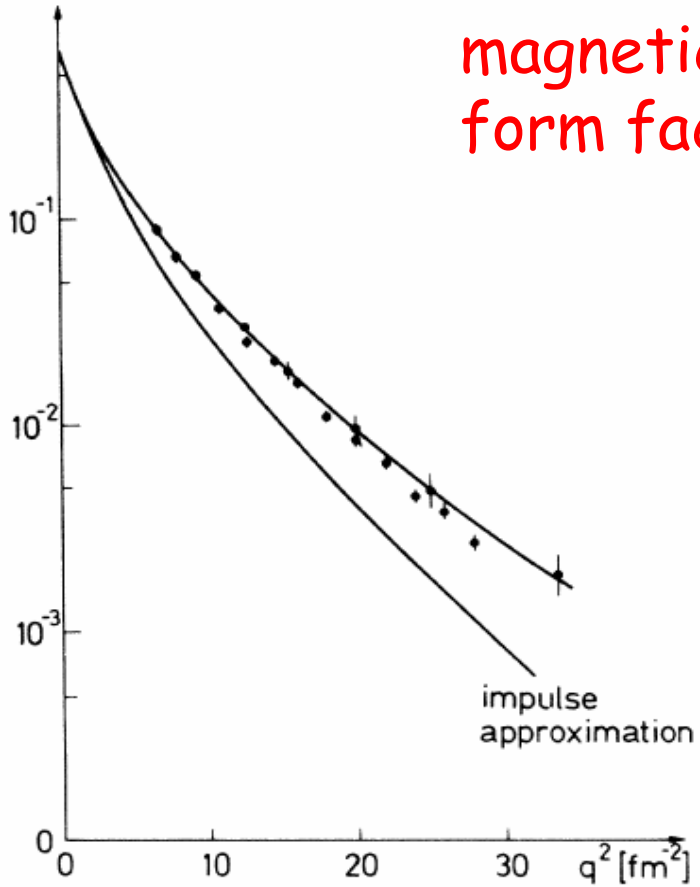

FIG. 2. Magnetic form factor of the deuteron vs momentum transfer. Shown is the contribution from the complete topological current well as that of the impulse approximation, where the exchange current contribution is neglected. The chiral angle has been determined from the isoscalar electric form factor of the single nucleon.

Exchange current
Identical in form
to ρ-π-γ current,
M. Wakamatsu,
W. Weise, NPA 477, 559
(1988)

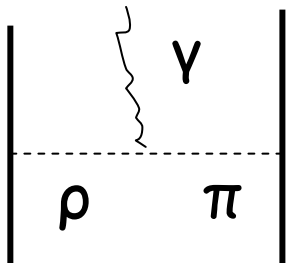

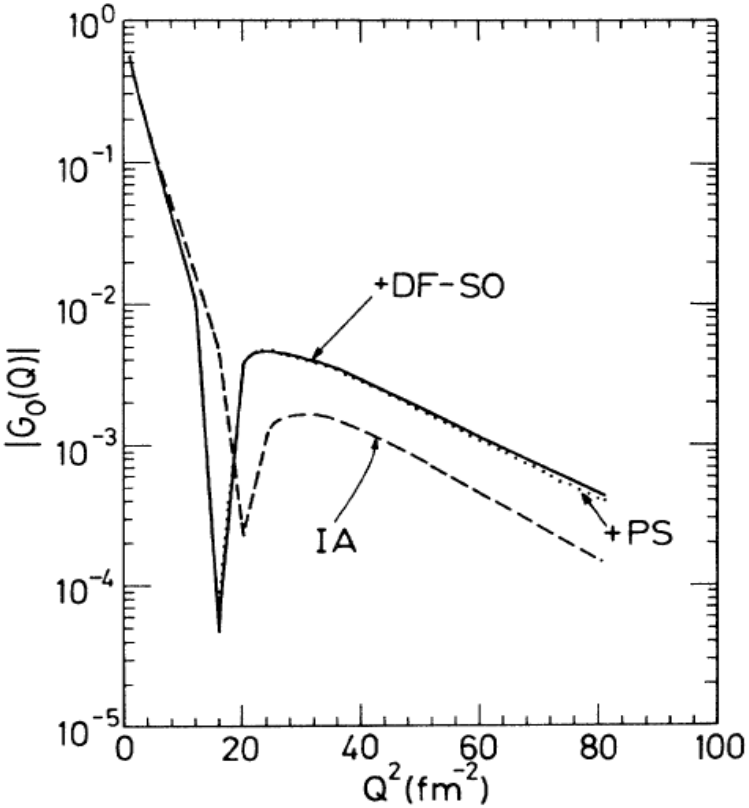

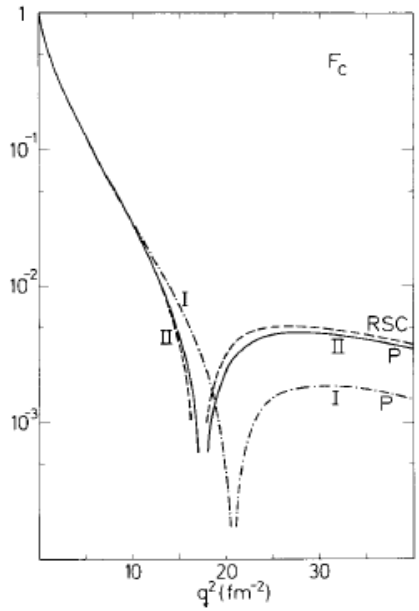

Fig. 5. The charge form factor of the deuteron using the chiral angle given by the dipole form for G_E^S. The curves I and II are the impulse approximation and complete results as obtained with the Paris-potential deuteron wavefunctions. The curve RSC is the result obtained with the Reid soft-core potential wavefunctions.

NUCLEAR WAVE FUNCTION
&
EXCHANGE CURRENTS

~

PRODUCT ANSATZ
SKYRME MODEL

Ground state solution with quantized rotational degrees of freedom

A. Acus et al, Phys. Scripta 69, 260 (2004)

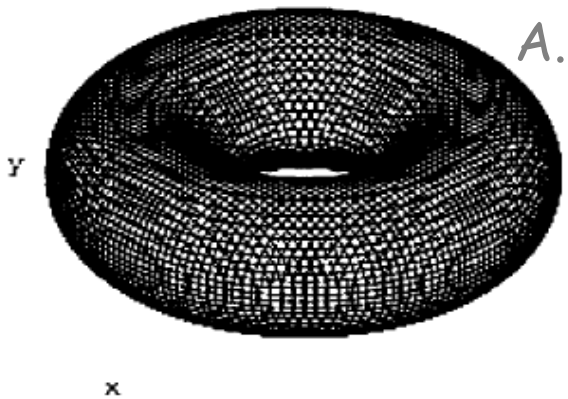

Equidensity

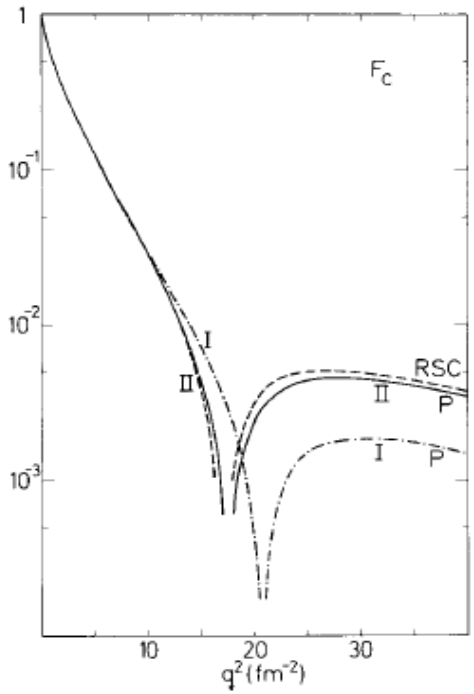

Fig. 5. The charge form factor of the deuteron using the chiral angle given by the dipole form for G_E^S. The curves I and II are the impulse approximation and complete results as obtained with the Paris-potential deuteron wavefunctions. The curve RSC is the result obtained with the Reid soft-core potential wavefunctions.

Product ansatz, EM Nyman, DOR 1987

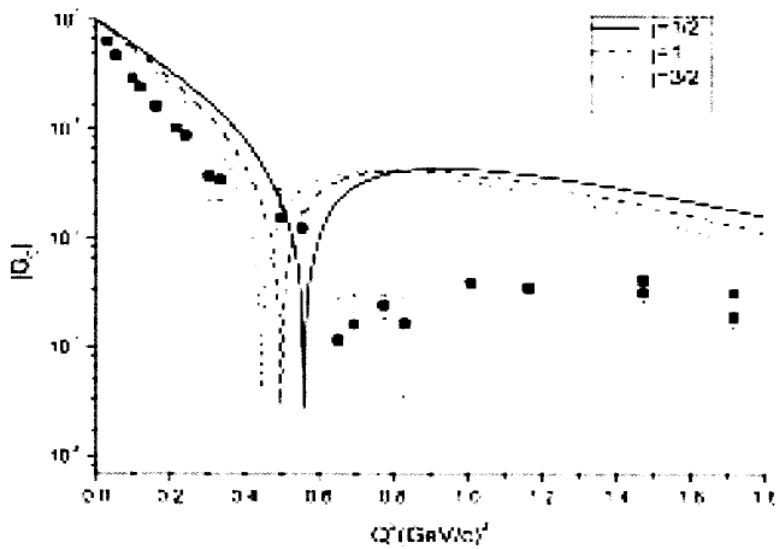

Fig. 3. Electric form factor of the quantized deuteron solution. The experimental data are from [16].

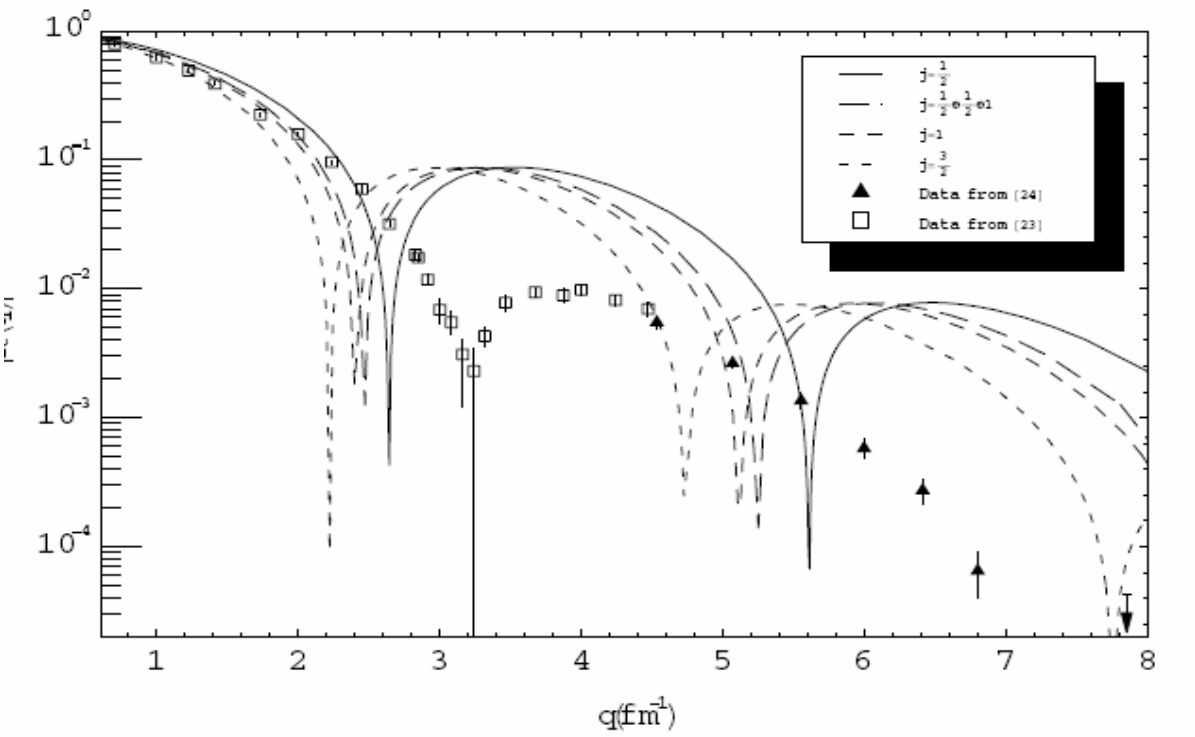

PRODUCT ANSATZ OVERSHOOTS!

A. Acus* and E. Norvaišas
D. O. Riska

PHYSICAL REVIEW C **74**, 025203 (2006)

FIG. 2. Comparison of ^{4}He electric form factors in different representations of SU(2) with experimental data [23,24]. The form factors are calculated with parameters that yield the experimental nucleon mass $m_N = 939$ MeV and radius $r = 0.72$ fm [11].

POINCARÉ INVARIANCE

WHY DOES PHOTONUCLEAR THEORY WORK ?

- ALMOST ALL PHOTO & ELECTRONUCLEAR FORMALISM EMPLOYS GALILEAN COVARIANT Q.M. WITH MINOR MODIFICATIONS DUE TO DIRAC SPINORS
- WHY ARE Q^2/M^2 EXPANSIONS NOT MISLEADING ?
- WHY DOESN'T THE QUARK MODEL PROVIDE A REALISTIC DESCRIPTION OF BARYON RESONANCE DECAYS?

GENERATORS OF POINCARÉ TRANSFORMATIONS

10 GENERATORS H, P_i, J_i, K_i

6 KINEMATIC GENERATORS, 4 SPECIFIED BY DYNAMICS THROUGH POINCARÉ ALGEBRA

3 ALTERNATIVES:

-INSTANT KINEMATICS P,J KINEMATIC O(3), E(3)*
-POINT KINEMATICS J, K KINEMATIC SO(1,3)
-FRONT KINEMATICS P, K KINEMATIC O(1,2)

* CONVENTIONAL, FIXED † HYPERPLANE

HAMILTONIAN: GALILEAN INVARIANCE ~
POINCARÉ INVARIANCE (LITTLE GROUP OF G AND P TRANSFORMATIONS COINCIDE)

CURRENTS: IN, OUT FRAME DIFFERENT: BOOSTS MATTER

EXAMPLE: FORM FACTORS
IN REST FRAME, BREIT FRAME $\sum p_i = \pm Q/2$

THE ROLE OF BOOSTS

INSTANT FORM:

$v = \pm p/\sum \omega_i$ $\quad v \sim Q^0$ boosts remain small

POINT FORM:

$v = \pm p/M$ $\quad v \sim Q^1$ boosts grow with Q

FRONT FORM:

Lightfront kinematics, boost invariant; spin dynamical

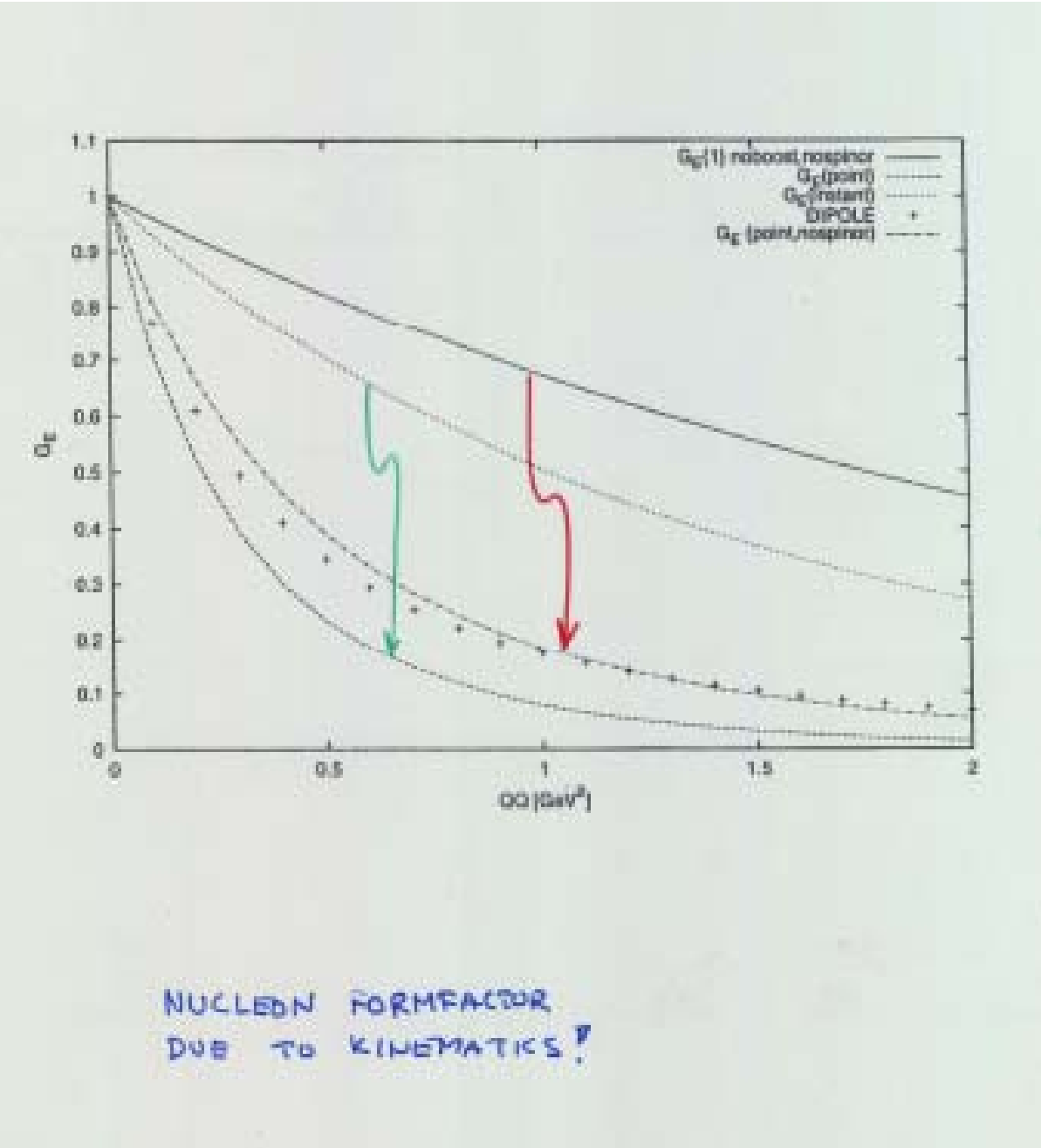

NUCLEON FORMFACTOR
DUE TO KINEMATICS!

IN POINT FORM THE NUCLEON FORM FACTOR ARISES FROM THE BOOST!

CHOICE OF KINEMATICS A MATTER OF PHENOMENOLOGICAL CONVENIENCE

NUCLEON FORM FACTORS IN THE QUARK MODEL IN 3 FORMS OF KINEMATICS, B.JULIA-DIAZ et al, PRC C69, 035212(2004)

SU(6) SPIN-ISOSPIN WAVEFUNCTION $\times$ $\varphi(P)$;

P = hypersperical momentum

$\varphi(P) \sim (1+P^2/4\ b^2)^{-a}$

	a	b (MeV)	matter radius (fm)
INSTANT	6	600	0.63
POINT	2.25	640	0.19
FRONT	4	500	0.55

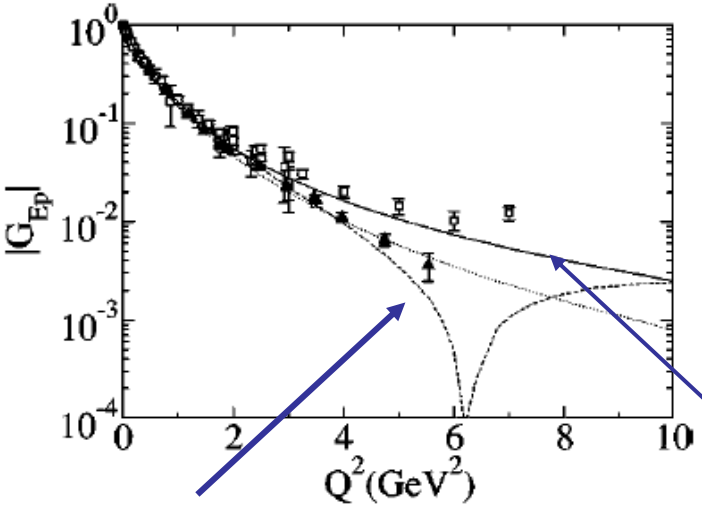

FRONT

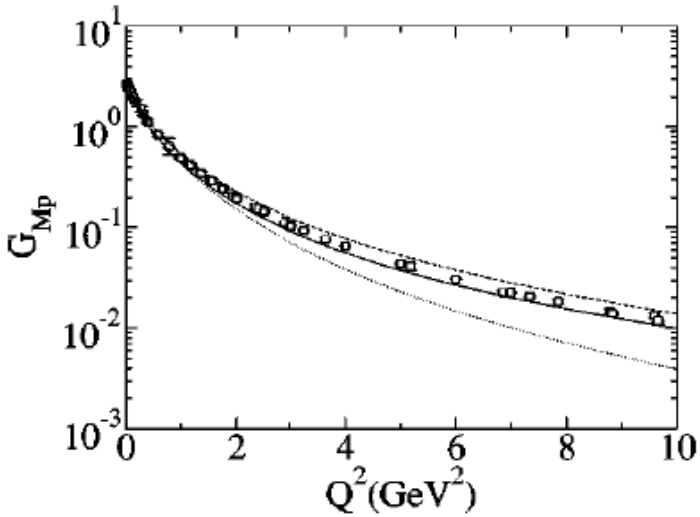

INSTANT

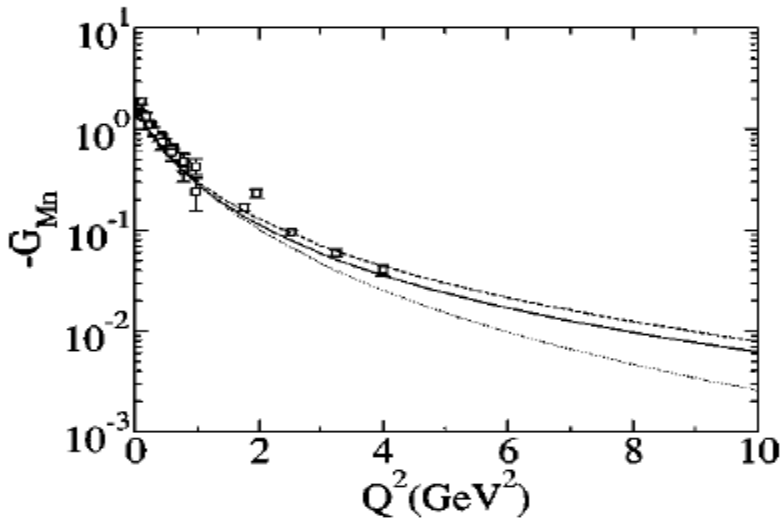

IF G_E HAS A NODE, FRONT FORM MAY BE OPTIMAL

$G_E(n)$

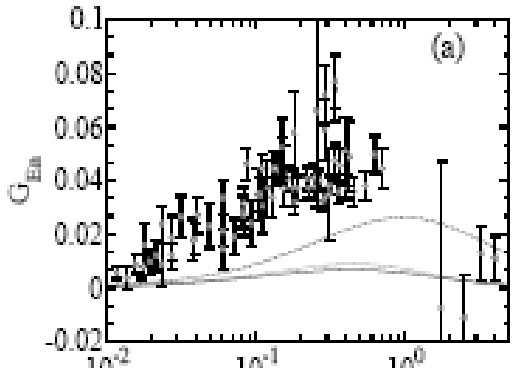

solid: instant, dotted: point
dashed: front

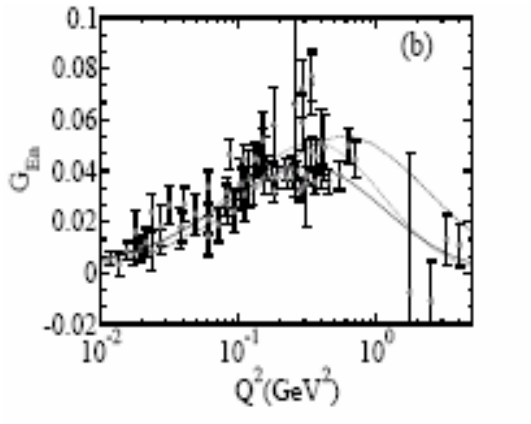

S′: 2% instant,point,
1% front

Consistent quark model demands covariant treatment of the boosts

1-2% mixed symmetry S-state
Sufficient to fix the qqq quark model

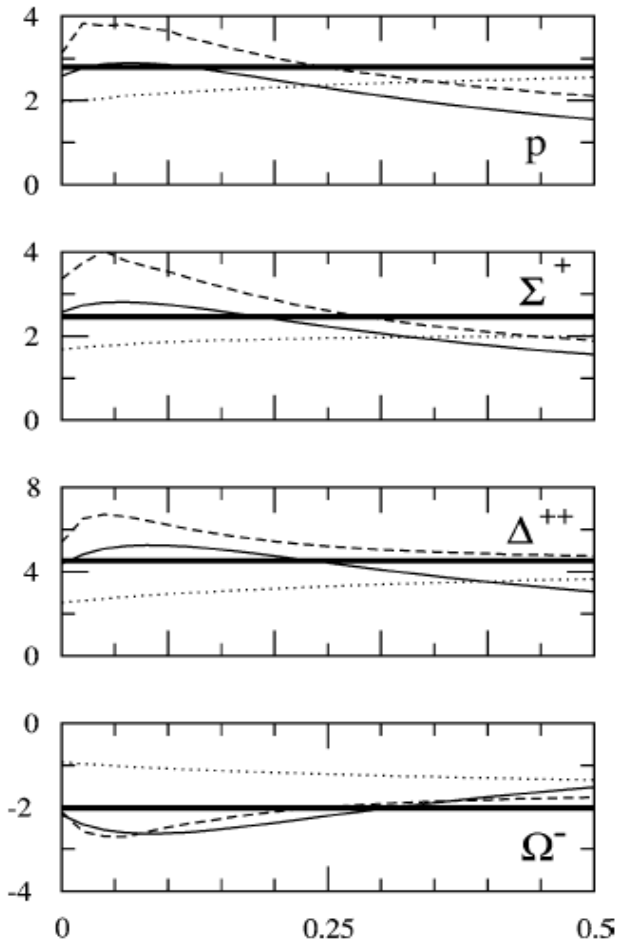

Fig. 1. Magnetic moments, in nuclear magnetons, of the p, Σ^+ and Δ^{++} as functions of the light constituent quark mass. The mass of the strange quark is fixed at 470 MeV for the Σ^+. Magnetic moment, in nuclear magnetons, of the Ω^- as a function of the mass of the strange quark. Solid, point and dashed lines correspond to instant, point and front forms of relativistic kinematics. The thick line corresponds to the experimental value.

FLAVOR ASYMMETRY IN THE PROTON

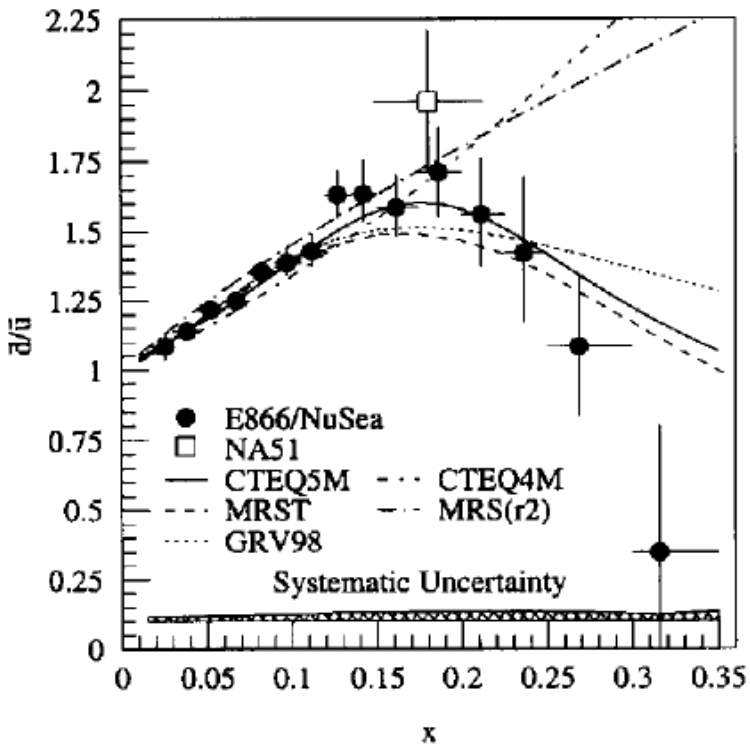

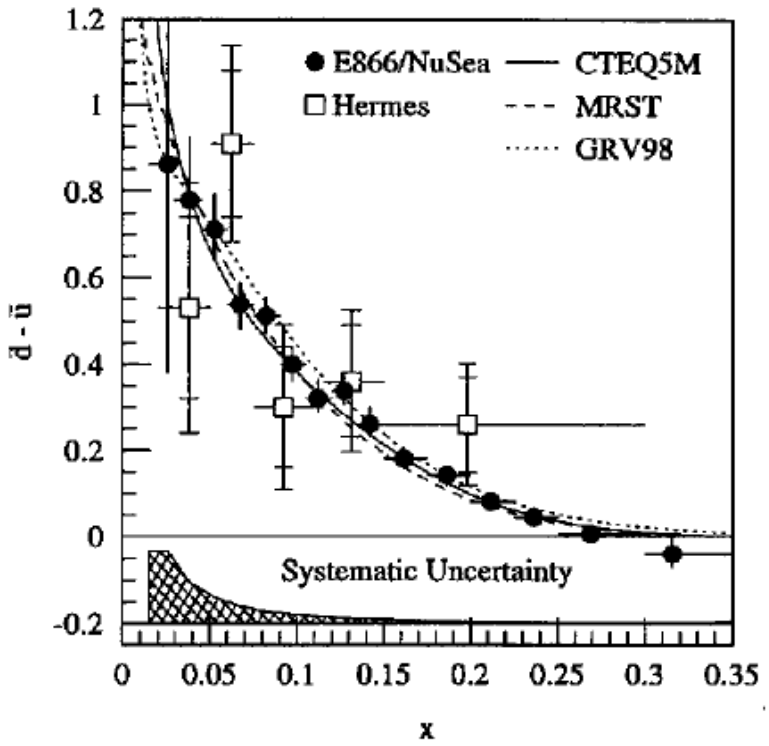

G.Garvey and J.C.Peng, Prog.Part.Nucl.Phys. 47, 203 (2001)

$d^- / u^- > 1$

$qqqq\bar{q}$ CONFIGURATIONS

qqqq SUBSYSTEM TOTALLY ANTISYMMETRIC

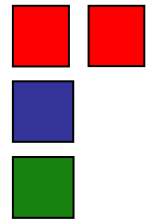

COLOR: [211] MIXED SYMMETRY (only 3 different colors)

SPACE-FLAVOR-SPIN: [31] MIXED SYMMETRY !

EITHER:

a) SPACE: SYMMETRIC [4], SPIN-FLAVOR: [31]

OR

b) SPACE: MIXED SYM: [31], SPIN-FLAVOR: [4]

1. SYMMETRIC SPATIAL WAVE FUNCTION: [4]

qqqq IN S-STATE, q^- IN P-STATE (q^- : - PARITY)

CORRESPONDS TO π – N OR K-HYPERON LOOP

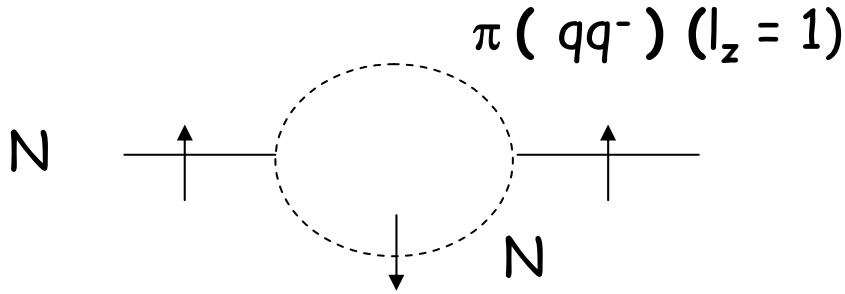

2. MIXED SYMMETRY SPATIAL WAVE FUNCTION: [31]

ONE QUARK IN P-STATE, q^- IN S-STATE

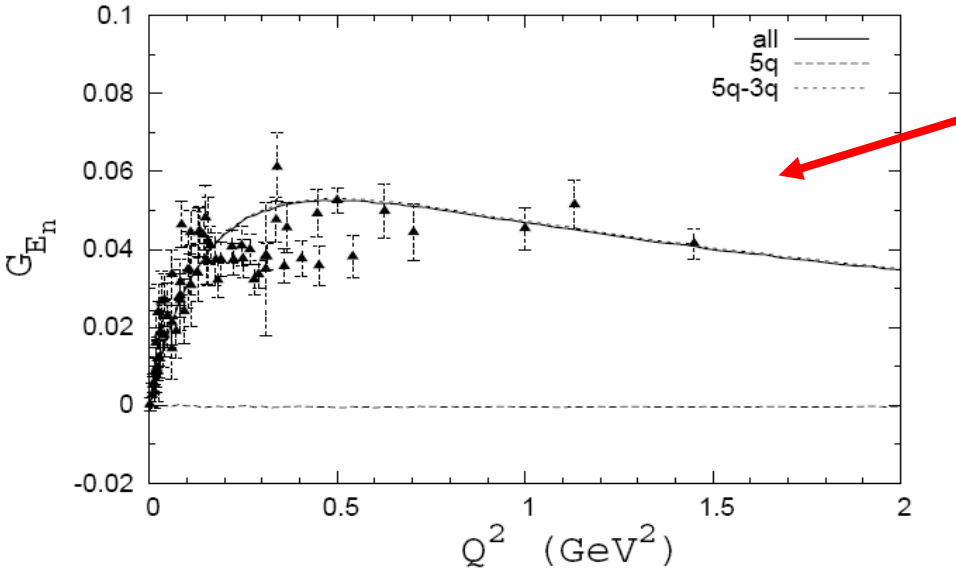

Antiquark in S-state
3% qqqqq$^-$

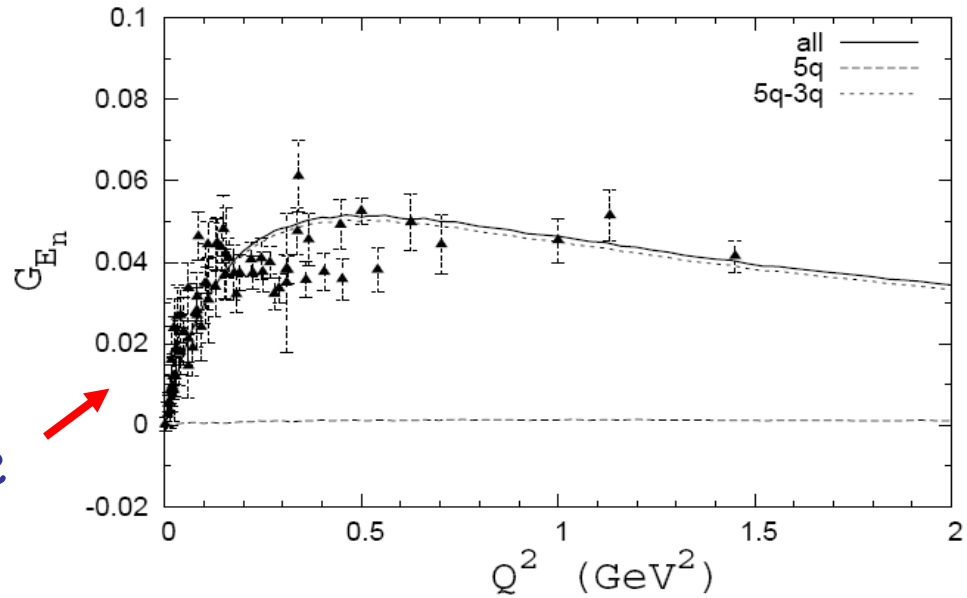

Antiquark in P-state
3% qqqqq$^-$

Qiang-Bing Li & DOR, nucl-th/0702049

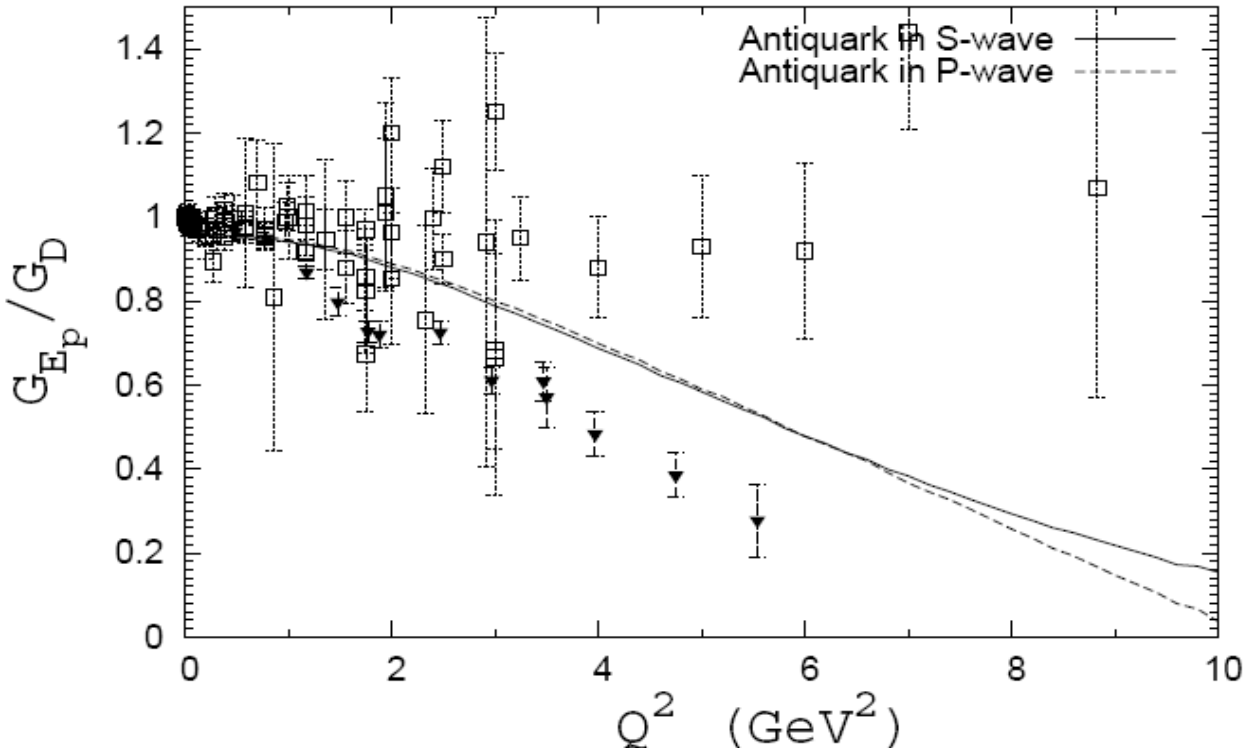
Antiquark in S-wave
Antiquark in P-wave
G_{E_p}/G_D
Q^2 (GeV^2)
0
0.2
0.4
0.6
0.8
1
1.2
1.4
0
2
4
6
8
10

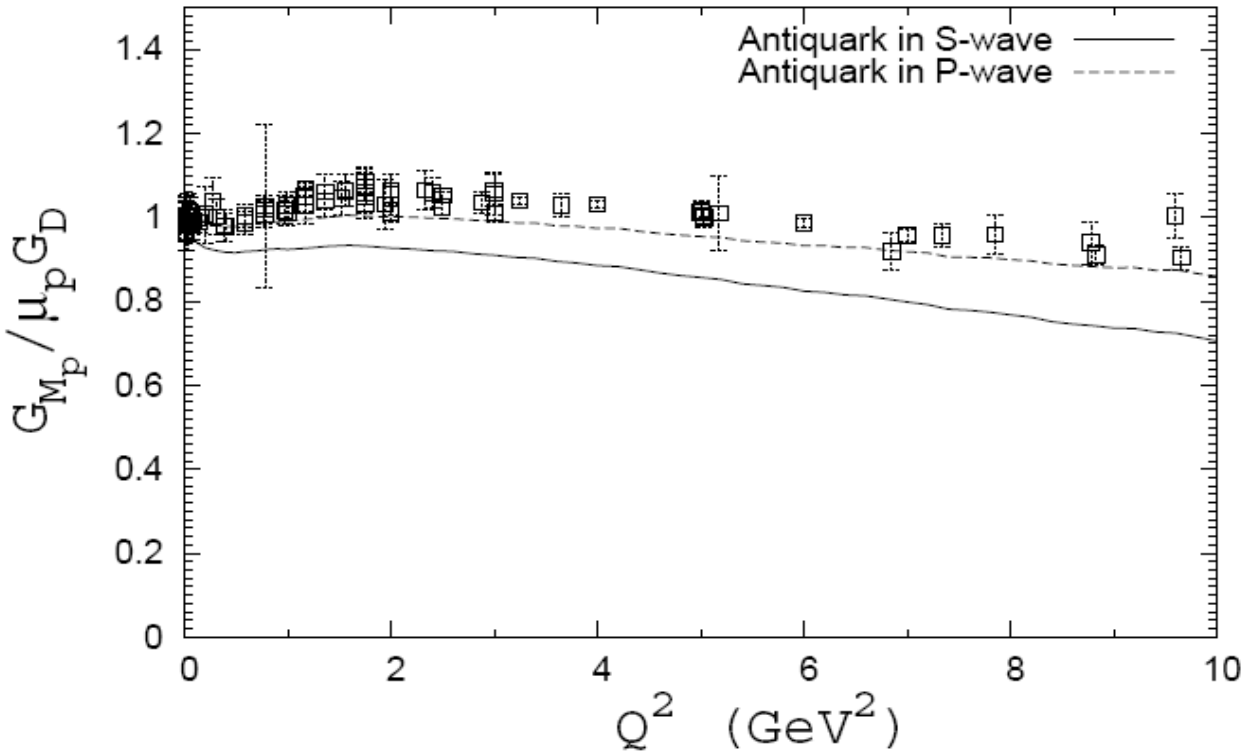
Antiquark in S-wave
Antiquark in P-wave
$G_{M_p} / \mu_p G_D$
Q^2 (GeV^2)
0
0.2
0.4
0.6
0.8
1
1.2
1.4
0
2
4
6
8
10

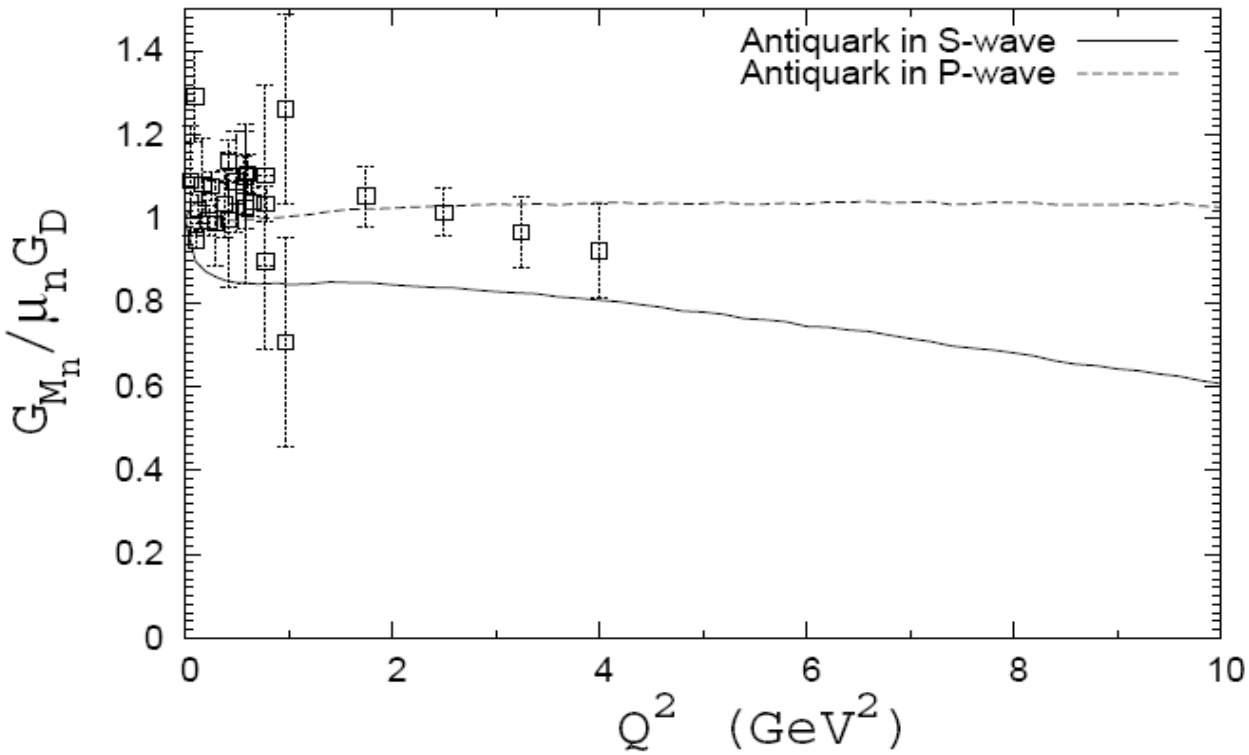
Antiquark in S-wave
Antiquark in P-wave
$G_{M_n} / \mu_n G_D$
Q^2 (GeV^2)
0
0.2
0.4
0.6
0.8
1
1.2
1.4
0
2
4
6
8
10

SUMMARY

- NUCLEAR OBSERVABLES ARE OFTEN MOST SENSITIVE TO LONG RANGE CHIRAL DYNAMICS
- THE SKYRMION LINKS LO CHIRAL DYNAMICS TO LARGE N QCD
- CHOICE OF POINCARÉ COVARIANT QUANTUM MECHANICS A MATTER OF CONVENIENCE
- UNQUENCHING OF THE QUARK MODEL SOLVE MANY PROBLEMS IN Q.M. PHENOMENOLOGY